J. Adv. Chem. Sci. - Volume 3 Issue 3 (2017) 499–501

ISSN: 2394-5311

Share Your Innovations through JACS Directory

Journal of Advanced Chemical Sciences

Visit Journal at http://www.jacsdirectory.com/jacs

Synthesis and Characterization of Bio-Template Assisted Lead Oxide Nanoparticles

R. Bapitha[1,2], M. Alagar[1,*]

[1]Department of PG Physics, Ayya Nadar Janaki Ammal College, Sivakasi - 626189, Tamil Nadu, India.
[2]Department of Physics, Sri Krishnasamy Arts and Science College, Mettamalai – 626 123, Tamil Nadu, India.

ARTICLE DETAILS

Article history:
Received 02 September 2017
Accepted 15 September 2017
Available online 26 September 2017

Keywords:
PbO Nanoparticles
Microwave Assisted Synthesis
Corn Starch
AC Impedance

ABSTRACT

A new attempt adopted to synthesize eco-friendly lead oxide nanoparticles. In the present work, uncapped and corn starch capped lead oxide nanoparticles were synthesized by microwave - assisted route. The results of XRD studies revealed that the synthesized lead oxide nanoparticles have high purity and crystallinity. The approximation method which is the theoretical method of calculating the particle size and microstrain of synthesized nanoparticles was successfully applied. The presence of Pb-O band in FT-IR spectrum affirmed that synthesized nanoparticles were lead oxide nanoparticles. The spherical shape of uncapped lead oxide nanoparticles were tuned to rod like shape due to addition of corn starch which was observed by SEM morphology analysis. The energy gap of synthesized nanoparticles was estimated from the UV-Vis absorption spectra of synthesized lead oxide nanoparticles. The higher value in energy gap of lead oxide nanoparticles than its bulk one, confirmed that the size of the synthesized particles were in nano range. The AC impedance studies have been performed to measure the grain boundary resistance of both capped and uncapped lead oxide nanoparticles.

1. Introduction

Nanostructure materials have received increasing attention in various fields in of science and technology. New synthetic routes for the preparation of ultrafine and nanosized metal oxides to obtain defined properties are under constant investigation and some of them include sol-gel, metal oxide chemical vapour deposition, co-precipitation, microemulsion by hydrolysis in polyol medium and decomposition of the precipitates prepared from non-aqueous precipitation routes [1].

Most of these techniques result in aggregation of nanoparticles during synthesis. Copolymer templates have been efficiently used to host chemical reaction. They have the advantage of avoiding nanoparticle clustering and also providing stable frameworks against chemical degradation. Use of copolymer templates has been reported for the synthesis of iron oxide Nanoparticles such as maghemite, cobalt ferrite and magnetite [2] and also for the synthesis of zinc oxide [3]. There is an increasing interest in the use of green resources for nanoparticle synthesis. Starch has been reported as a capping agent during the precipitation of iron oxide through the precipitation of ferric salts as its hydroxide using triethylamine or by precipitating a mixture of ferric and ferrous salts [2]. Rice starch has been used as bio-template to synthesize zinc oxide Nanoparticles through hydrothermal-biotemplate method using zinc-acetate sodium hydroxide and uncooked rice flour at various ratios as precursors at 120 °C for 18 hours [3]. Polysaccharides have also been employed to modify the surface characteristics of nano iron oxides generated [2].

Lead oxide is an important industrial material due to its unique electronic, mechanical and optical properties and its potential applications in nanodevices and functionalized materials such as active materials of lead acid batteries, valve-regulated lead acid batteries and lithium secondary batteries. Because of the simplicity of design, low cost of manufacturing, reliability and relative safety when compared to other electrochemical systems of lead - acid batteries, there is a high interest to improve and develop lead oxide characteristics to obtain more discharge capacity and more cycle life [4]. Due to their unique properties lead oxides have wide applications such as network modifiers in luminescent glassy materials, pigments, gas sensors, paints, storage batteries and nanoscale electronic devices [5].

*Corresponding Author
Email Address: alagaranjac@yahoo.co.in (M. Alagar)

2. Experimental Methods

2.1 Materials

Lead (II) nitrate, ammonia solution and corn starch are obtained from Fisher and Merck Company.

2.2 Methods

The microwave-assisted route is used to synthesis lead oxide nanoparticles for various surfactants/capping agent. The capping agent corn starch was added to100 mL of 0.1 M of lead nitrate solution. Then the solution was stirred well till the polymers were dissolved in the solution completely. After that 20 mL of ammonia solution was added and stirred it for 30 minutes. The mixed solution was placed in microwave oven for 2 min with a power of 640 W and 15 min with a power of 329 W. A considerable amount of white precipitate obtained. After cooling to room temperature, the precipitate was filtered, washed with de-ionized water and the absolute ethanol, and dried at room temperature for 3 days. The dry product was annealed at 400 °C for 2 hrs. Finally orange lead oxide nano powder was obtained.

2.3 Characterization

X-ray diffraction (XRD) measurements are carried out with XPERT-PRO System. The FTIR spectra are recorded by a SHIMADZU-8400S, FTIR Spectrometer, in the region of 400-4000 cm^{-1}, with a signal average of 20 scans at a resolution of 4 cm^{-1}. UV-Vis studies are recorded by a SHIMADZU-2606, UV-Vis Spectrometer. Conductivity studies are carried out by an AC impedance analyzer Newton's 4th Ltd UK, Model PSM 1735.

3. Results and Discussion

3.1 XRD Studies

X-ray diffractogram of synthesized PbO nanoparticles are shown in Fig. 1. From the Fig. 1, the observed sharp and narrow peaks illustrate that all the samples possessed high crystallinity [3].

Cite this Article as: R. Bapitha, M. Alagar, Synthesis and characterization of bio-template assisted lead oxide nanoparticles, J. Adv. Chem. Sci. 3(3) (2017) 499–501.

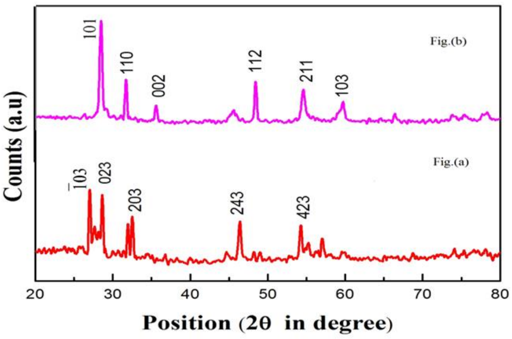

Fig. 1 XRD Pattern of (a) lead oxide, (b) lead oxide-corn starch

The diffraction peaks of uncapped lead oxide nanoparticles may be indexed to a monoclinic phase of $Pb_{12}O_{19}$ (JCPDS card no: 19-0697) while all the diffraction peaks of corn starch capped lead oxide may be indexed as a tetragonal phase of PbO (JCPDS card no: 05-0561).

The estimated crystallite size of the samples, in various orientations, from their corresponding XRD details are tabulated in Tables 1 and 2. The average crystallite size for each sample is also tabulated in Table 3. Polymeric structure of starch with helical shaped carbonaceous matrix which carrying multiple polyol groups create a protective and functionalized surrounding shield for metal ions which plays a structure directing role. So it can have the capable of changing the crystal structure of the uncapped PbO nanoparticles. As the diffraction depends on crystal structure, the XRD pattern of (b) is not matched with (a) and also it is the reason for not agreeing of phase index of corn starch capped lead oxide nanoparticles with uncapped one.

Table 1 Uncapped lead oxide

Position (θ)(angle)	FWHM (radian)	d-Spacing	hkl	Crystallite size (nm)
13.513	0.003142	3.29658	1 3 0	45.39
14.32515	0.003142	3.11327	0 2 3	45.54
16.28015	0.003142	2.74779	2 0 3	45.97
23.1965	0.006283	1.95564	2 4 3	24.00
27.13115	0.006283	1.68914	4 2 3	24.79

Table 2 Lead oxide-corn starch surfactant

Position(θ) (angle)	FWHM (radian)	d-Spacing	hkl	Crystallite size (nm)
14.23885	0.006283	3.13175	1 0 1	22.77
15.8603	0.004189	2.81858	1 1 0	34.41
17.80585	0.006283	2.51903	0 0 2	23.18
24.23455	0.005236	1.87661	1 1 2	29.04
27.2803	0.008378	1.68061	2 1 1	18.62
29.82055	0.016755	1.54901	1 0 3	9.54

Table 3 Comparison of size of uncapped and corn starch capped lead oxide nanoparticle

System	Average crystallite size (nm)
Lead oxide(uncapped)	37.13
Lead oxide - corn starch	22.92

The crystallite size is decreased by ~15 nm from its uncapped lead oxide nanoparticles. It may be due to the zeta potential of the template. A large negative zeta potential was found to be advantageous for achieving lower particle sizes, owing to the particles remaining discrete without agglomeration [6]. Zeta potential was evaluated by a dynamic light scattering technique. Where the corn starch template provided for capping or encapsulation to keep the synthesized nanoparticles separate, this work employs the templates to provide binding sites for the Pb^{2+} centers, which are then spatially separated and thus can be effectively synthesized to lower sizes by controlled removal of the template. These Pb^{2+} centers are subsequently converted to the corresponding oxide by controlled chemical reaction and heat treatment [2]. Among all the bio-templates, it was seen that the crystallinity of lead oxide nanoparticles are improved by the addition of corn starch.

3.2 SEM Analysis

Morphology of each samples were studied by SEM. The obtained results are shown in Fig. 2. In the case of uncapped lead oxide nanoparticles, agglomerations of many primary particles are formed (Fig. 2). Slightly agglomerated rod like shape is observed in corn starch capped lead oxide nanoparticles (Fig. 2b). The morphology of lead oxide nanoparticles is improved while corn starch used as a capping agent. Finally it can be interpreted as during nucleation the controlled growing mechanism was taken place during corn starch used as capping agent.

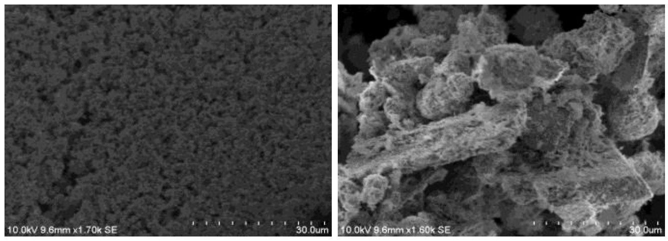

(a) (b)

Fig. 2 a) Lead oxide (no capping agent) - uncapped lead oxide nanoparticles and b) lead oxide – corn starch - corn starch capped lead oxide nanoparticles

3.3 UV-Vis Spectrum Analysis

UV-Vis absorption spectroscopy is an efficient technique to monitor the optical properties of quantum sized particles. The energy gap between valence and conduction band is of fundamental importance for the properties of a solid. Most of a material's behaviors, such as intrinsic conductivity, optical transitions, or electronic transitions depend on it. The energy gap is changed by reducing crystallite size. In addition, affects such as structural changes, lattice construction, atomic relaxation, surface reconstruction, surface passivation or strain induced by a host material [7].

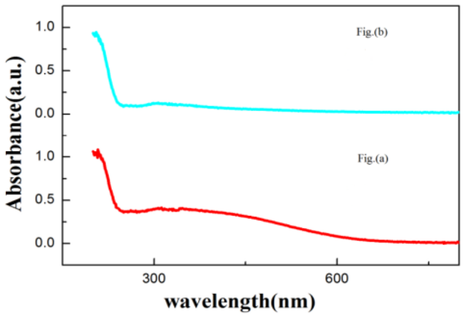

Fig. 3 UV-Vis absorption spectra of (a) lead oxide, (b) lead oxide-corn starch

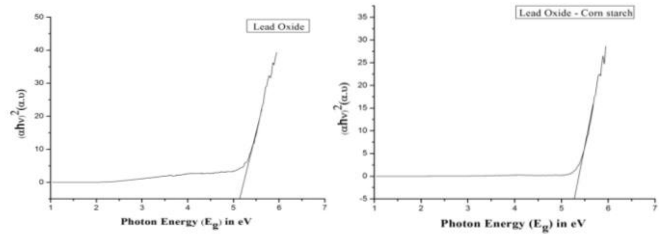

(a) (b)

Fig. 4 Plot of linear portion of $\alpha h\nu^2$ versus hν for a) lead oxide (b) lead oxide-corn starch

The band gap(E_g) can be calculated from the Eq.,

$$(\alpha h\upsilon)^n = B(h\upsilon - E_g)$$

where α is the absorption coefficient, hν is the photon energy, B is a constant characteristic to the material and n equals either ½ for an indirect transition or 2 for a direct transition. Fig. 3 shows the UV-Vis absorbance spectrum of the synthesized samples. $\alpha h\nu^2$ versus hν curve shown in Fig. 4. The value of hν extrapolated to α=0 gives the absorption band gap energy [8]. The energy gap values of all the samples are tabulated in Table 4.

Table 4 Comparison of energy gap

Samples	Energy gap (eV)
Lead oxide	5.1448
Lead oxide-corn starch	5.2727

Then the corn starch capped lead oxide nanoparticles have high energy gap value than the uncapped one. The energy gap values of the synthesized two samples are higher than its bulk nanoparticles [9]. The increase in the band gaps can be related to the quantum confinement effects and/or small size effects of the lead oxide nanoparticles [10].

3.4 FT-IR Studies

In order to understand the mechanism of formation of lead oxide nanoparticles and related changes occurring in the particle size, an infra-red spectroscopic measurement of lead oxide nanoparticles in the absence and presence of surfactants was carried out.

FT-IR spectra of all samples are shown in Fig. 5. In the FT-IR spectrum of uncapped lead oxide nanoparticles the -OH stretching peaked at 3315.41 cm^{-1}, 3141.82 cm^{-1}, 3128.32 cm^{-1} and 3026.10 cm^{-1} [11]. The shoulder at 1400 cm^{-1} is due to the vibrations of strong bonding of oxygen with lead. The confirmation peaks for the presence of lead oxide in the synthesized nanoparticles is observed at 655.55 cm^{-1} and 490.31 cm^{-1} [12, 13]. In the FT-IR spectrum of lead oxide-corn starch, the confirmation peak of Pb-O band arises at 655.55 cm^{-1} and 464.16 cm^{-1}. The Pb-O band at 490.31 cm^{-1} is disappeared because of the influence of corn starch bio-template. The assignments for all other frequencies shown in Table 5.

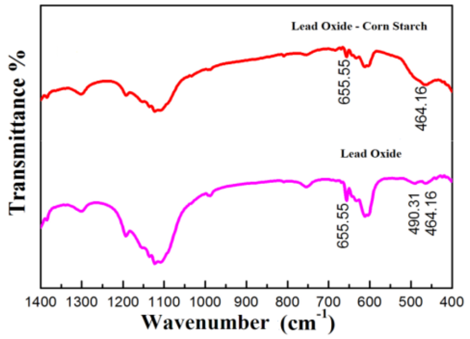

Fig. 5 FT-IR Spectrum of capped/uncapped lead oxide nanoparticles

Table 5 List of vibrational modes and its corresponding assignments

Vibrational mode (cm^{-1})	Assignments
3377.12	-OH stretching
1404.08	Angular deformation of CH bond in starch molecule
754.19	Entire anhydroglucose ring stretch in starch

3.5 AC Impedance

The four prepared samples were made into pellets and placed in between the electrodes. Frequency 1 Hz - 1 MHz is applied to uncapped and PVP, PVA capped lead oxide nanoparticles and 30 Hz to 10 MHz is applied to corn starch capped lead oxide nanoparticles for zero bias voltage. The AC impedance spectroscopy has been used to investigate the effect of capping agents such as PVP, PVA and corn starch on the electrical property of Lead Oxide nanoparticles. Typical impedance spectra for capped and uncapped lead oxide nanoparticles are shown in Fig. 6. All the spectra contain only a single arc. Accordingly, the semicircle at high and low frequencies may be assigned to charge transport within the crystallites and a grain boundary effect, respectively. In general, the grain boundary effect on electrical conductivity may originate from a grain boundary potential barrier or from space charge layers which are depleted in majority charge carriers and which are localized along the grain boundaries. However, a low frequency semicircle may also be an artifact caused by porosity, which is known as the constriction effect [14, 15]. In the present work, the obtained single arc corresponding to low frequency is attributed to the grain boundary resistance. Some authors thought that the one arc spectrum means that the conduction process through the grain and the grain boundary had identical time constants, $\tau=1/\omega=RC$, in which ω,R and C are peak frequency of the impedance arc, the resistance and the capacitance. This means that the conduction in the grain and grain boundary occurs in the same process, so they cannot be separated by the impedance spectroscopy. Other authors thought that the single arc was interpreted as due to the contribution from the grain boundary based on the model having resistive grain boundaries and conducting grain cores [16, 17].

The resistance values estimated from the Cole-Cole plot is of the order of 10^7 Ω and hence it may be concluded that the calculated resistance values are of lead oxide grain boundaries according to thought of later authors. It is evident from the Fig. 6 that the additions of various capping agents have altered the shape of the impedance spectrum of uncapped lead oxide nanoparticles. The intersection between the arc and the real axis in the low frequency region represents the total dc resistance of the sample [18]. The grain boundary resistances estimated from the impedance plots are given in Table 6. It can be concluded that the electrical properties of each lead oxide sample may be depend on its grain size [16].

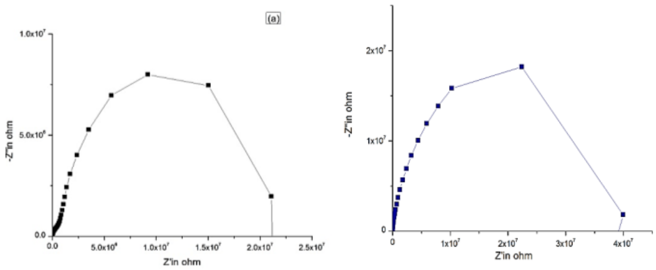

Fig. 6 Impedance Spectra of (a) lead oxide, (b) lead oxide-corn starch at 0V

Table 6 Comparison of grain boundary resistance

System	Grain boundary resistance $\times10^8$ in Ω at 0V
Lead oxide(uncapped)	2.109
Lead oxide-corn starch	3.999

4. Conclusion

Corn starch capped and uncapped lead oxide nanoparticles were synthesized by microwave assisted method. The XRD results show that there is a size confinement with the change in surfactants. Morphology of PbO nanoparticles were tuned well while corn starch used as capping agents. From the UV-Vis absorption spectra, high energy gap value was obtained for corn starch capped PbO nanoparticles due to small size effects and quantum confinement effects. From the FT-IR spectrum of the samples, the influences of surfactants were affirmed. Variation in grain boundary resistance of PbO nanoparticles was observed at zero bias voltage, through AC impedance study for different capping agents. The highest grain boundary resistance was seemed in the case of corn starch capped PbO nanoparticles due to small grain size.

References

[1] A. Lagashetty, V. Havanoor, S. Basavaraja, S.D. Balaji, A. Venketaraman, Microwave-assisted route for synthesis of nanosized metal oxides, Sci. Technol. Adv. Mat. 8 (2007) 484-493.

[2] S.K. Janardhanan, I. Ramasamy, B. Unni Nair, Synthesis of iron oxide nanoparticles using chitosan and starch templates, Trans. Met. Chem 33 (2008) 127-131.

[3] D. Ramimoghadam, M. ZobirBin Hussein, Y.H. Taufiq-Yap, Hydrothermal synthesis of zinc oxide nanoparticles using rice as soft biotemplate, Chem. Cent. J. 7(136) (2013) 1-10.

[4] M.K. Mahmoudabad, M.M.K. Motlagh, Synthesis and characterization of PbO nanostructure and NiO doped with PbO through combustion of citrate/nitrate gel, Int. J. Phys. Sci. 6(24) (2011) 5720-5725.

[5] S. Gnanam, V. Rajendran, Optical properties of capping agents mediated lead oxide nanoparticles via facile hydrothermal process, Int .J. Nanomat. BioStruct. 1(2) (2011) 12-16.

[6] M. Nidhin, R. Indumathy, K.J. Sreeram, B. Unni Nair, Synthesis of iron oxide nanoparticles of narrow size distribution on polysaccharide templates, Bull. Mater. Sci. 31(1) (2008) 93-96.

[7] H.S. Nalwa, Hand book of thin films materials, Vol. 5, Elsevier, 2007

[8] G. Wang, X. Shen, J. Horvat, Bei Wang, Hao Liu, David Wexler, Hydrothermal synthesis and optical, magnetic, and supercapacitance properties of nanoporous cobalt oxide nanorods, Phys. Chem. C 113 (2009) 4357-4361.

[9] S.A. Aly, M.A. Kaid, N.Z. El-Sayed, Some optical aspects of thermally evaporated lead oxide thin films, Physica. Polonica. A 124 (2013) 713-716.

[10] S. Farhadi, J. Safabakhsh, P. Zaringhadam, Synthesis, characterization, and investigation of optical and magnetic properties of cobalt oxide (Co3O4) nanoparticles, J. Nanostr. Chem. 3(69) (2013) 1-9.

[11] M. Kottaisamy, D. Jeyakumar, Jegannathan, M. Rao, Yttrium oxide:Eu^{3+} red phosphor by self-propagating high temperature synthesis, Mater. Res. Bull. 31 (1996) 1013-1020.

[12] V. Timer, R.L. Ciceo, I. Ardelean, Structural studies of iron doped B_2O_3.0.7PbO.0.3Ag_2O glasses by FT-IR and Raman spectroscopies, Semicond. Phys. Quant. Elect. Optoelect.11 (2008) 221-225.

[13] S. Li, W. Yang, M. Chen, J. Gao, J. kang, Y. Qi, Structural and electrochemical characterization of $LiMn_{2-\delta}V_{\delta}O_y$ spinels, Mat. Chem. Phys. 90 (2005) 261-269.

[14] J.E. Bauerle, Study of solid electrolyte polarization by a complex admittance method, J. Phys. Chem. Solids 30 (1969) 26572670.

[15] J. Fleig, J. Maier, Finite-element calculations on the impedance of electroceramics with highly resistive grain boundaries: I, Laterally inhomogeneous grain boundaries, J. of Am. Ceram. Soc. 82 (1999) 3485–3493.

[16] C.W. Nan, A.T. Schope, S. Holten, H. Kliem, Grain size-dependent electrical properties of nanocrystalline ZnO, J. Appl. Phys. 85 (1999) 7735.

[17] Z. Zhou, K. Kato, T. Komaki, M. Yoshino, H. Yukawa, M. Morinaga, K. Morita, Effects of dopants and hydrogen on the electrical conductivity of ZnO, J. Eur. Ceram. Soc. 24 (2004) 139-146.

[18] Z. Zhou, K. Kato, T. Komaki, M. Yoshino, H. Yukawa, M. Morinaga, K. Morita, Electrical conductivity of Cu-Doped ZnO and its Change with hydrogen implantation, J. Electroceram.11 (2003) 73-79.